3 Characterization and Design of Microbubble-Based Contrast Agents Suitable for Diagnostic Imaging

Eleanor Stride

CONTENTS

3.1 Introduction

The benefits of coated microbubble-based contrast agents in ultrasound (US) image enhancement have been clearly demonstrated since the development of the first commercial agents in the 1970s. More recently, their potential use in therapeutic applications such as targeted drug delivery has also become an active area of research. However, existing theoretical descriptions of coated microbubble are inadequate in several respects and despite considerable investigation, coated microbubbles behaviour is by no means fully understood. There is consequently substantial scope for improving the effectiveness of contrast agents, and despite a lack of definite evidence for harmful effects, there inevitably remain some concerns as to their safety.

E. Stride, PhD
Department of Mechanical Engineering, University College London, Torrington Place, London, WC1E 7JE, UK

The aim of this chapter is to discuss the deficiencies in coated microbubble characterisation and examine how these may be addressed in order to improve contrast agent design.

3.1.1 Contrast Agent Design

The first step in any design process is to define the requirements for a particular application. In the case of diagnostic imaging, the aim is to obtain a satisfactory image of the region of interest, quickly, safely and, if possible, economically. In terms of equipment costs and portability, scanning time and patient risk, US is superior to alternative imaging techniques such as CT and MR imaging. In terms of image quality, however, it is generally inferior, and the requirement for a contrast agent is to lessen this disadvantage by increasing the reflectivity of a particular feature compared with that of the surrounding tissue.

Gas microbubbles are effective contrast agents because their presence vastly increases the difference in acoustic impedance between the normally liquid filled blood vessels and the neighbouring solid or semi-solid tissue. There is, in addition, a fortuitous coincidence between the frequency range over which coated microbubbles resonate and that which is used in diagnostic imaging, and under the right conditions, coated microbubbles will exhibit significantly non-linear behaviour. This can be exploited very effectively for imaging, as will be described below. Thus, whilst the discovery of microbubble contrast agents was in fact accidental (Gramiak and Shah 1968), in design terms, they represent an ideal choice for US contrast enhancement.

In therapeutic applications the aim is to target treatment, be it a drug or a physical effect such as heating, to a specific region of the body in order to minimise unwanted side effects. There is a wider range of factors to consider in assessing the optimality of microbubbles for this purpose than for

contrast enhancement. For example, in addition to ensuring the survival of the microbubbles in vivo, the microbubble coating may be required to act as an anchor site for certain species according to the type of therapy to be delivered and/or the target area.

There may also be differing requirements regarding the shape of coated microbubbles. Spheres have a low ratio of surface area to volume, whereas to increase the probability of a particle adhering to a target, a large surface area is desirable. Notwithstanding the question of optimality, however, coated microbubbles are undoubtedly an effective means of delivering therapy, particularly if there is an additional requirement for imaging, for example to trace the passage of the coated microbubbles to the target site. They can also be destroyed using US, which enables treatment to be delivered directly to the target site.

3.1.2 Aims and Requirements

Having established the suitability of microbubbles for diagnostic and therapeutic applications in a general sense, the design of the coated microbubbles themselves must now be examined more closely to identify areas for improvement. The precise requirements will naturally vary according to the application and, for the purposes of illustration, the following discussion will therefore concentrate upon coated microbubble design for image enhancement. The procedure may easily be adapted for therapeutic applications however.

The three main requirements for an US contrast agent are:

- Detectability – Coated microbubbles should produce as large a contrast effect as possible for a given dose.
- Longevity – Coated microbubble survival times should be sufficient to enable imaging of the required region.
- Safety – Coated microbubbles should pose no risk to the patient.

For existing contrast agents these are conflicting requirements. In order to achieve a large contrast effect, and thereby minimise the dose required, the scattered signal from the coated microbubbles must be distinct from that generated by tissue. At present, the most effective way of obtaining a distinctive signal is to use a high acoustic power of insonation (high mechanical index, MI). This not only increases the amplitude of the signal and the proportion of coated microbubbles excited, but also causes the microbubbles to behave non-linearly. In theory, the non-linear components in the overall scattered signal will be due primarily to this behaviour. Thus, by using an appropriate imaging technique such as pulse inversion (Chap. 4), which isolates these components, much of the noise from the surrounding tissue can be eliminated. However, using a high acoustic power also increases the likelihood of coated microbubble destruction. This may be desirable for certain types of imaging, but it requires larger and/or more frequent doses to be administered and is clearly unacceptable if, for example, drug carrying coated microbubbles are being imaged away from the target site. Moreover, at high acoustic power the potential for harmful bio-effects is necessarily increased, and the effects of non-linear propagation through the surrounding tissue will become noticeable, thus limiting the maximum microbubble/tissue signal ratio that may be achieved.

The possibility of designing coated microbubbles in order to overcome this problem is discussed in Sect. 3.2. There are some further requirements to consider first however. These are general to all applications.

An ideal coated microbubble should:

- Respond predictably and reproducibly
- Have a well defined destruction threshold
- Locate preferentially in the area required
- Be economical to produce
- Be convenient to administer
- Eventually disintegrate or be eliminated from the body

The reproducibility of coated microbubble response, the ease with which coated microbubbles can be administered and their cost, will be determined primarily by the manufacturing process. It should perhaps be noted at this point that the main disadvantage of ultrasound contrast agents is the fact that the need to administer them increases the time, skill and resources required for performing a scan. Since this must be offset against the benefits of contrast agents, it is important that manufacturing requirements are considered in the design process.

As indicated above, the ability of coated microbubbles to "locate preferentially", whether for imaging or treatment, is related primarily to their surface chemistry, as is their ability to disintegrate and/or be eliminated from the body. These properties will be discussed further in Sect. 3.3. To predict either

the acoustic response or the destruction threshold of a coated microbubble, an accurate model is required. This is also the principle requirement for determining the most important factors on which to concentrate for design. The development of a suitable model is the subject of the next section.

3.2 Modelling and Analysis

3.2.1 Derivation of a General Model

A number of models describing the response of a single, coated gas microbubble to an imposed US field have been developed (Fox and Herzfeld 1954; Glazman 1983; Lord et al. 1990; de Jong et al. 1992; Church 1995; Khismatullin and Nadim 2002; Morgan et al. 1999). They vary in terms of their complexity but, regardless of the rigour with which they were originally derived, they can be shown to be mathematically equivalent. In the absence of reliable experimental data it is not possible to assess their relative worth. The following discussion will therefore be based on a generalised model, of which the models mentioned above represent specific forms.

A spherical volume of gas enclosed by a stabilising outer layer and suspended in a volume of liquid is considered (Fig. 3.1). The notation used is defined in Table 3.1. The validity of the assumptions underlying the model will be assessed subsequently. For the present, spherical symmetry is assumed and conservation of momentum in spherical polar coordinates yields:

$$\rho\left(\frac{\partial u}{\partial t}+u\frac{\partial u}{\partial r}\right)+\frac{\partial p}{\partial r}=\frac{\partial T_{rr}}{\partial r}+\frac{2T_{rr}-T_{\theta\theta}-T_{\phi\phi}}{r} \tag{3.1}$$

Similarly, from conservation of mass:

$$\frac{\partial \rho}{\partial t}+\rho\frac{\partial u}{\partial t}+u\frac{\partial \rho}{\partial r}+\frac{2\rho u}{r}=0 \tag{3.2}$$

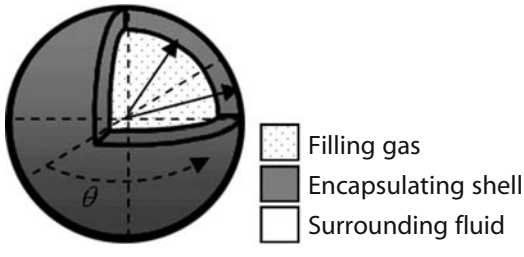

Fig. 3.1. The coated microbubble system considered

Table 3.1. Notation

Symbol	Definition	Subscript	Definition
u	radial velocity	r	radial
t	time	G	gas
p	pressure	S	shell
T	stress	L	liquid
r	radial coordinate	1	inner surface
R	radius	2	outer surface
R	radial velocity	∞	conditions at infinity
R	radial acceleration	o	initial conditions
f	factor	v	viscous
V	volume	s	stiffness
G	shear modulus	*rad*	radiation
M	strain time derivative	*th*	thermal
d	thickness	A	acoustic
k	constant	e	equilibrium conditions
		max	maximum
δ	damping factor	*min*	minimum
σ	surface tension	θ	latitudinal
ω	frequency	ϕ	longitudinal
μ	viscosity		
κ	polytropic constant		
ψ	material function		
τ	time variable		
α	material constant		
Γ	concentration		
χ	elasticity parameter		
ρ	density		

Integrating Eq. 3.1 over three regimes for the gas, shell and surrounding fluid gives:

$$\begin{aligned}&\int_0^{R_1}\left[\rho_G\left(\frac{\partial u}{\partial t}+u\frac{\partial u}{\partial r}\right)+\frac{\partial p}{\partial r}-\frac{\partial T_{G,rr}}{\partial r}-\frac{2T_{G,rr}-T_{G,\theta\theta}-T_{G,\phi\phi}}{r}\right]dr\\&+\int_{R_1}^{R_2}\left[\rho_S\left(\frac{\partial u}{\partial t}+u\frac{\partial u}{\partial r}\right)+\frac{\partial p}{\partial r}-\frac{\partial T_{Srr}}{\partial r}-\frac{2T_{S,rr}-T_{S,\theta\theta}-T_{S,\phi\phi}}{r}\right]dr\\&+\int_{R_2}^{\infty}\left[\rho_L\left(\frac{\partial u}{\partial t}+u\frac{\partial u}{\partial r}\right)+\frac{\partial p}{\partial r}-\frac{\partial T_{L,rr}}{\partial r}-\frac{2T_{L,rr}-T_{L,\theta\theta}-T_{L,\phi\phi}}{r}\right]dr=0\end{aligned} \tag{3.3}$$

The density, elasticity and viscosity of the filling gas will be considerably smaller than those of the solid shell or surrounding fluid, particularly at the low insonation pressures which are of most interest in this discussion. The first integral may therefore be neglected. If the surrounding fluid is considered to be infinite, i.e. the presence of boundaries such blood vessel walls and other coated microbubbles is ignored, there is no need to modify the third integral.

If the presence of other coated microbubbles in the fluid is ignored, then, at the relevant frequencies and radial amplitudes, the speed of the coated microbubble wall (≈5 m/s) will be much smaller than the speed of sound in either the shell or the surrounding fluid (≈1500 m/s). ρ_s and ρ_L may therefore be treated as constants and hence from Eq. 3.2:

$$u(r,t)=\frac{R_1^2(t)\dot{R}_1(t)}{r^2} \tag{3.4}$$

From conservation of radial stress on either side of the shell:

$$p_G(R_1,t) = p_S(R_1,t) - T_{S,rr}(R_1,t) + \frac{2\sigma_1}{R_1} \tag{3.5}$$

$$p_S(R_2,t) - T_{S,rr}(R_2,t) = p_L(R_2,t) - T_{L,rr}(R_2,t) + \frac{2\sigma_2}{R_2} \tag{3.6}$$

Surface tension has been treated as a constant in Eqs. 3.5 and 3.6 since, as will be shown in Sect. 3.3, the elastic effect due to variation in the concentration of surface molecules can be included in the definition of $T_{s,rr}(R_{1or2}, t)$. It has also been assumed that the vapour pressure inside the coated microbubble will be negligible.

Substituting into Eqs. 3.4–3.6 gives:

$$\rho_S\left(R_1\ddot{R}_1 - R_1\ddot{R}_1\frac{R_1}{R_2} + \frac{3}{2}\dot{R}_1^2 - \left(\frac{4R_2^3 - R_1^3}{2R_2^3}\right)\frac{\dot{R}_1^2R_1}{R_2}\right) + \rho_L\left(\left(\frac{4R_2^3 - R_1^3}{2R_2^3}\right)\frac{\dot{R}_1^2R_1}{R_2} + R_1\ddot{R}_1\frac{R_1}{R_2}\right)$$
$$= \left(p_G - p_\infty(t) - \frac{2\sigma_1}{R_1} - \frac{2\sigma_2}{R_2} + \int_{R_1}^{R_2}\left[\frac{2T_{S,rr} - T_{S,\theta\theta} - T_{S,\phi\phi}}{r}\right]dr + \int_{R_2}^{\infty}\left[\frac{2T_{L,rr} - T_{L,\theta\theta} - T_{L,\phi\phi}}{r}\right]dr\right)$$

This may be rewritten as:

$$R_1\ddot{R}_1\left(1 + \left(\frac{\rho_L - \rho_S}{\rho_S}\right)\frac{R_1}{R_2}\right) + \dot{R}_1^2\left(\frac{3}{2} + \left(\frac{\rho_L - \rho_S}{\rho_S}\right)\left(\frac{4R_2^3 - R_1^3}{2R_2^3}\right)\frac{R_1}{R_2}\right)$$
$$= \frac{1}{\rho_S}\left(p_G - p_\infty(t) - \frac{2\sigma_1}{R_1} - \frac{2\sigma_2}{R_2} + f_{Ls} + f_{Ss} + f_{Lv} + f_{Sv} + f_{\delta_{rad}} + f_{\delta_{th}}\right) \tag{3.7}$$

f_{Sv}, f_{Ss}, f_{Lv} and f_{Ls}, correspond to the integrals for stress in the shell and fluid. The two additional factors, $f_{\delta rad}$ and $f_{\delta th}$, represent respectively the damping of coated microbubbles oscillations due to the reradiation of the sound field and that due to conduction from the filling gas to the surroundings. The rigorous derivation of these last two terms will be discussed later. In its present form Eq. 3.7 represents a generalised model for coated microbubble behaviour. The existing models differ only in the way in which the last six terms are defined.

3.2.2 Sensitivity Analysis

Before seeking to define f_{Sv}, f_{Ss}, f_{Lv}, f_{Ls}, $f_{\delta rad}$, $f_{\delta th}$, p_G and p_∞, it is desirable to identify which factors are the most significant in controlling coated microbubble behaviour, and hence which areas are the most important for modelling and design. It is therefore necessary to make some preliminary simplifying assumptions from which initial definitions of the above terms can be derived.

Firstly, if the assumption that the surrounding fluid is incompressible is retained for the present, then $f_{drad} = 0$. If it also assumed that the fluid is purely Newtonian then:

$$f_{Ls} = 0 \quad \text{and} \quad 2T_{\theta\theta} = 2T_{\phi\phi} = -T_{rr} = T_{L,rr} = 2\mu_l\frac{\partial u}{\partial r}$$

and hence

$$f_{Lv} = 3\int_{R_2}^{\infty}\frac{T_{L,rr}}{r}dr = -4\mu_l\frac{R_1^2\dot{R}_1}{R_2^3}$$

Similarly, if the shell is assumed to be a homogeneous, linear viscoelastic solid layer having finite thickness, then for small strain:

$$f_{Ss} = \frac{-4G_S(R_1 - R_{1e})\left(R_2^3 - R_1^3\right)}{R_2^3R_1} \text{ and, } f_{Sv} = -4\mu_S\dot{R}_1\left(\frac{R_2^3 - R_1^3}{R_2^3R_1}\right)$$

For these conditions it is justifiable to assume that gas behaviour will be polytropic and since coated microbubbles are unlikely to be perfectly gas-tight, the gas pressure at equilibrium may be taken to be equal to the ambient pressure p_o.

Thus $p_G(R_1,t) = p_o\left(\frac{R_{o1}}{R_1}\right)^{3\kappa}$ and $f_{\delta th} = 0$.

The maximum coated microbubble diameter is restricted by the size of the smallest human blood vessels to approximately 8 μm. For the range of frequencies used in diagnostic imaging (1–10 MHz) this will be at least an order of magnitude smaller than the wavelength of the incident sound field. In the absence of any other coated microbubbles or neighbouring boundaries therefore, the incident pressure may be considered to be uniform over the surface of the coated microbubble. At low acoustic power of insonation, distortion due to non-linear propagation will be small and, for the purposes of this preliminary analysis, the incident field may be modelled as a simple sinusoid $p_\infty(t) = p_o + p_A\sin(\omega t)$.

Substituting from the above into Eq. 3.7 gives:

$$R_1\ddot{R}_1\left(1 + \left(\frac{\rho_L - \rho_S}{\rho_S}\right)\frac{R_1}{R_2}\right) + \dot{R}_1^2\left(\frac{3}{2} + \left(\frac{\rho_L - \rho_S}{\rho_S}\right)\left(\frac{4R_2^3 - R_1^3}{2R_2^3}\right)\frac{R_1}{R_2}\right)$$
$$= \frac{1}{\rho_S}\left(p_o\left(\frac{R_{o1}}{R_1}\right)^3 - p_o - p_A\sin(\omega t) - \frac{2\sigma_1}{R_1} - \frac{2\sigma_2}{R_2} - \frac{4\dot{R}_1R_1^2\mu_L}{R_2^3} - \frac{4\dot{R}_1V_S\mu_S}{R_2^3R_1} - \frac{4V_SG_S}{R_2^3}\left(1 - \frac{R_{1e}}{R_1}\right)\right) \tag{3.8}$$

This is equivalent to the form derived by Church (1995).

To determine the factors having the most significant effect upon coated microbubble behaviour, Eq. 3.8 may be rearranged once again in terms of wall acceleration $\ddot{R}_1$, and broken down into seven components representing: the filling gas pressure (*PF*), the inertia of the shell and surrounding fluid (*IF*), the incident pressure (*AF*), surface tension (*SF*), fluid viscosity (L_vF), shell viscosity (S_vF), and shell stiffness (S_sF).

$$\ddot{R}_1 = PF + IF + AF + TF + L_vF + S_vF + S_sF$$

$$\ddot{R}_1 = \underbrace{\frac{P_o}{A}\left(\frac{R_{o1}}{R_1}\right)^3}_{PF} - \underbrace{\frac{\rho_S \dot{R}_1^2}{A}\left(\frac{3}{2}+\left(\frac{\rho_L-\rho_S}{\rho_S}\right)\left(\frac{4R_2^3-R_1^3}{2R_2^3}\right)\frac{R_1}{R_2}\right)}_{IF} - \underbrace{\frac{p_o + p_A Sin(\omega t)}{A}}_{AF}$$
$$- \underbrace{\frac{2}{A}\left(\frac{\sigma_1}{R_1}+\frac{\sigma_2}{R_2}\right)}_{TF} - \underbrace{\frac{4\dot{R}_1 V_S \mu_S}{AR_1R_2^3}}_{L_vF} - \underbrace{\frac{4\dot{R}_1 R_1^2 \mu_L}{AR_2^3}}_{S_vF} - \underbrace{\frac{4V_S G_S}{AR_2^3}\left(1-\frac{R_{1e}}{R_1}\right)}_{S_sF}$$

$$A = \rho_S R_1\left(1+\left(\frac{\rho_L-\rho_S}{\rho_S}\right)\frac{R_1}{R_2}\right) \tag{3.9}$$

This type of analysis is similar to that carried out by Flynn (1964) to investigate the nature of free bubble cavitation behaviour.

Equation 3.9 may either be solved numerically or else linearised to enable an analytical solution. Since ultimately it is the non-linear behaviour of coated microbubbles which is of interest for design, a numerical approach is preferable. The size of the acceleration factors may then be compared and their relative importance determined. This type of analysis also enables the sensitivity of coated microbubble behaviour to variation in the model parameters to be assessed as shown in the next section.

3.2.3 Results and Implications

Figure 3.2 shows plots of the acceleration factors for a coated microbubble and a free microbubble of the same size exposed to the same insonation conditions. These were obtained for the parameters shown in Table 3.2 according to the procedure described in Stride and Saffari (2003). The shell parameters were selected to be of the same order of magnitude as those obtained for commercial contrast agents (de Jong et al. 1992; Gorce et al. 2000). For reasons that will be explained subsequently, the fluid parameters used were those of plasma and it was assumed that the gas would behave ideally and isothermally. A variety of insonation frequencies were used, corresponding to resonant, sub-resonant and super-resonant regimes. Figure 3.2 shows the case for 3 MHz at which the radial amplitude was maximised. The relative magnitude of the different components of Eq. 3.9 was similar at all frequencies however. The insonation pressure was varied within the range of pressures (0.05–0.1 MPa) at which it would be reasonable to expect a coated microbubble to remain intact (Stride and Saffari 2003) and for which Eq. 3.9 would be valid.

Table 3.2. Simulation parameter values

	Parameter	Symbol	Value	Unit
Gas (air) Cengel and Boles (1989)	Polytropic constant	κ	1.0	
	Ambient pressure	p_o	0.1	MPa
Shell (Albunex) Church (1995)	Shear modulus	G_s	88.8	MPa
	Density	ρ_s	1100	Kgm^{-3}
	Viscosity	μ_s	1.77	Pas
	Inner radius	R_1	3.635	μm
	Thickness	d_e	15	nm
	Inner surface tension	σ_1	0.04	Nm^{-1}
	Outer surface tension	σ_2	0.005	Nm^{-1}
Liquid (plasma) Duck (1990)	Density	ρ_l	1030	Kgm^{-3}
	Viscosity	μ_l	0.0015	Pas

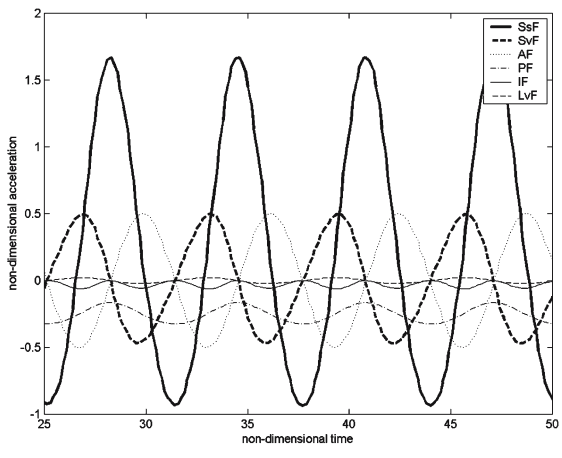

a

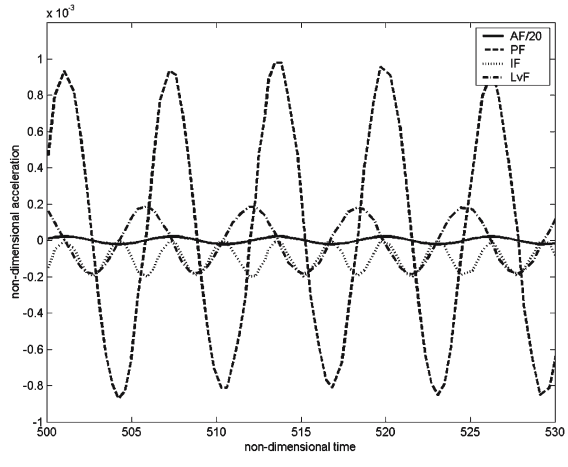

b

Fig. 3.2a,b. Acceleration factors for (a) an Albunex-coated microbubble and (b) a free bubble insonified at 3 MHz and 50 kPa. Factors TF and L_vF have been omitted in (a) and (b), respectively, as they have negligible amplitude.

A comparison of Fig. 3.2a and Fig. 3.2b indicates that the factors controlling the behaviour of a coated microbubble may differ considerably from those controlling the behaviour of a free bubble. Whilst the latter is primarily determined by either pressure or inertia, microbubble response is dominated by the stiffness and viscosity of the encapsulating shell. This finding has a number of implications. For example, it calls into question the validity of relating results obtained from work on free bubbles to coated microbubbles. This is particularly relevant for the assessment of contrast agent safety, which has in many cases been based on results derived from free bubble models (Nyborg 2001). For the purposes of design, the main conclusion is the importance of the shell as an area requiring accurate modelling and offering opportunities for modifying coated microbubble response. Similarly, the relatively large amplitude of the incident pressure factor indicates that the sound field should also be a focus for modelling and design.

Figure 3.3 indicates the sensitivity of coated microbubble radial acceleration to a change of ±20% in each of the variables shown in Table 3.2. The results suggest that, as might be expected, coated microbubble response is most sensitive to changes in the shell and sound field parameters (G_s, m_s, d_s, f, p_A). This reinforces the finding from Fig. 3.2 that these factors are the most significant in terms of coated microbubble design.

Before the modelling and/or design of the shell and sound field can be considered further, the validity of the sensitivity analysis itself must be examined. The results of the analysis present something of a paradox: the aim of the sensitivity analysis is to determine which parts of the model it is most important to improve. In order to perform the analysis however, a model is required which, by implication, must be inferior. It is therefore necessary to re-examine the assumptions made above and determine under which circumstances the sensitivity analysis could be invalidated.

The first point to examine is the model of the filling gas. Potentially, a different model could increase the relative amplitude of *PF* in Eq. 3.9. However, at the small amplitudes of oscillation considered, the temperatures and pressures inside the coated microbubble would be, respectively, high and low compared with the critical values for the gas, and deviation from ideal gas behaviour would be expected to be minimal. Secondly, if the stiffness and viscosity of the shell were much lower than those given in Table 3.2, or if the shell was damaged so that its influence were lessened, then coated microbubble behaviour would be expected to be closer to that of a free bubble. At present, however, it is only shells having a strong influence upon coated microbubble behaviour at non-destructive insonation pressures that are of interest for the purposes of design.

The justification for ignoring fluid compressibility has already been given. An additional term taking account of the elasticity of the surrounding fluid could be included in Eq. 3.8. However, for fluids such as plasma, and indeed for whole blood, the size of this term is so small compared with the shell elasticity that its influence upon coated microbubble dynamics is negligible (Stride and Saffari 2004). For coated microbubbles enclosed in narrow blood vessels and/or other types of denser, stiffer tissue, the non-Newtonian behaviour of the surroundings may be more significant and require careful modelling (Allen and Roy 2000). The validity of the sensitivity analysis is therefore restricted to the behaviour of coated microbubbles in relatively large blood vessels. Fortunately, for the application of diagnostic imaging, this is frequently a reasonable assumption.

A similar analysis could be carried out for different coated microbubble applications again by examining the equations describing the relevant physical processes and identifying the controlling factors. In the case of coated microbubble acoustic response, the most important factors were found to be the encapsulating shell and the sound field. For controlling the long term stability of coated microbubbles on the other hand, the diffusivity of the gas is likely to be important as well as the permeability and solubility of the shell. Some of these considerations will be discussed again later. The next section considers modelling and engineering coated microbubbles to control and improve their acoustic response.

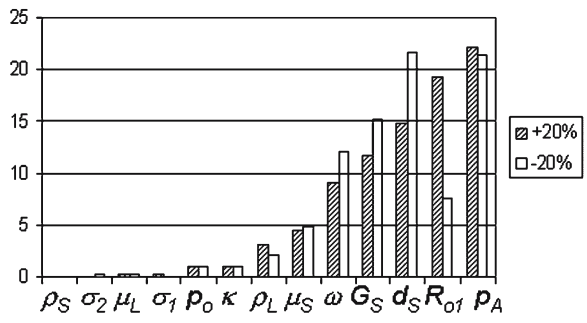

Fig. 3.3. The sensitivity of coated microbubble wall radial acceleration to variations of ±20% in each of the model parameters shown in Table 3.2 for insonation at 1 MHz and 50 kPa

3.3 Design and Engineering

There are two types of variables involved in the design and engineering of coated microbubbles. Firstly, there are those which, within limits, can be controlled, such as the shell, the gas and the sound field. Secondly, there are those, such as the surrounding fluid, which cannot be controlled but whose influence upon coated microbubble behaviour must be considered since it may affect the design requirements.

3.3.1 The Encapsulating Shell

The conclusion from the preceding analysis was that the main determinant of response is the encapsulating shell. It is therefore important that its behaviour should be modelled correctly, not only to enable coated microbubble response to be accurately predicted, but also to indicate the most effective means of engineering the shell to achieve a particular response. To do this, the assumptions underlying the modelling of the shell must be reviewed to determine their validity.

3.3.1.1 Improving the Shell Model

It was assumed above that coated microbubble behaviour would be spherically symmetric. On the basis of optical studies by Postema et al. (2003) this assumption would appear to be incorrect. In terms of coated microbubble acoustic response, however, the effect of asymmetric behaviour would be expected to be relatively small. The decay rate for the pressure wave generated by aspherical oscillations will be very rapid compared with that for the wave due to radial pulsations (Leighton 1994). For the purposes of this study therefore, it is justifiable to retain the assumption of sphericity and thereby confine the analysis to one dimension.

It was also assumed in deriving Eq. 3.8 that the shell was of finite thickness and consisted of a homogeneous, linear viscoelastic solid. This too may be seen to be invalid. A simple linear model is inappropriate if decisions regarding the optimum shell material are to be made. A fairly wide range of materials has been used for coating microbubbles, from palmitic acid to cyanoacrylate. Thus, even if it is justifiable to regard some materials as behaving linearly at low amplitudes of oscillation, this may not be the case in general. Moreover, some shell materials are far more fluid in nature than others and it may be more appropriate to consider them as liquids or as two-dimensional layers, i.e. having negligible thickness, than as solid shells.

Considering firstly non-linear viscoelastic behaviour: it cannot be assumed in this case that the trace of the stress tensor **T** in Eq. 3.3 will be zero and the shell functions will therefore be of the form

$$f_{Ss} + f_{Sv} = 2\int_{R_1}^{R_2} \frac{T_{S,rr} - T_{S,\theta\theta}}{r}\, dr$$

Again spherical symmetry has been assumed so that $T_{\phi\phi} = T_{\theta\theta}$.

There are several models available for describing this type of material. One of the most general is that due to Green and Rivlin (1957).

$$\mathbf{T}(t) = \int_{-\infty}^{t} \left\{\mathbf{I}\psi_1 tr(\mathbf{M}_1) + \psi_2 \mathbf{M}_1\right\} d\tau_1 + \int_{-\infty}^{t}\int_{-\infty}^{t} \left\{\mathbf{I}\psi_3 tr(\mathbf{M}_1) tr(\mathbf{M}_2) + \mathbf{I}\psi_4 tr(\mathbf{M}_1\mathbf{M}_2) + \mathbf{I}\psi_5 tr(\mathbf{M}_2) + \psi_6 \mathbf{M}_1\mathbf{M}_2\right\} d\tau_1 d\tau_2 + \ldots \tag{3.10}$$

where $\tau_{1,2}$ are time variables of integration, **I** is the identity matrix and $\mathbf{M}_{1,2}$ are the time derivatives of the strain tensor with respect to $\tau_{1,2}$, etc. Functions $\psi_{1,2}$, etc. must be determined experimentally for a particular material. Incorporating Eq. 3.10 into Eq. 3.7 generates a system of differential equations which can be solved numerically. This form of Eq. 3.7 is also suitable for modelling large amplitude deformations.

The next case to consider is that of a surfactant layer. It has already been shown that there may be a significant difference between the behaviour of a free bubble and an encapsulated microbubble (Fig. 3.2). The nature of a surfactant coated microbubble is currently unclear in this respect. According to the results obtained by Gorce et al. (2000) the shell parameters for phospholipid monolayers are of the same order of magnitude as those obtained for albumin shells. However, results reported by Postema et al. (2003) suggest that phospholipids-coated microbubbles behaviour is closer to that of a free bubble. Further controlled experiments are required to resolve this discrepancy.

It is undoubtedly true, however, that the material microstructure is different for surfactants and polymers. A phospholipid monolayer for example, consists of a single layer of molecules bound together by secondary (Van de Waals) bonds. These are continuously broken and reformed, with the result that the

molecules can "slip" over each other, allowing the layer to deform without wrinkling. Polymers such as serum albumin, on the other hand, consist of much larger intertwined molecular chains which may be cross-linked by covalent bonds. This prevents continuous deformation so that the shell is more likely to buckle and/or rupture. In both cases, resistance to tension and compression is due to intermolecular forces opposing the movement of molecules from their equilibrium positions. However, given the monomolecular thickness of the surfactant layer, it may be more appropriate to treat this resistance as a variation in surface tension of a single interface, rather than as the elasticity of a finite solid layer as is appropriate for thicker polymer shells.

The boundary condition (Eq. 3.5) for a single interface with a surfactant layer may be expressed as:

$$p_G(R,t) = p_L(R,t) - T_{L,rr}(R,t) + \frac{2\sigma}{R} + \frac{\partial\sigma}{\partial R} + \frac{1}{R^3}\frac{\partial\alpha}{\partial R} - \frac{\alpha}{R^4}$$

where σ is surface tension and α is a parameter relating to repulsion between molecules.
The corresponding form of Eq. 3.7 is:

$$\rho_L\left(R\ddot{R} - R\ddot{R}_1 + \frac{3}{2}\dot{R}_1^2\right) = \left(p_G(R,t) - p_\infty(t) - \frac{2\sigma}{R} - \frac{\partial\sigma}{\partial R} - \frac{1}{R^3}\frac{\partial\alpha}{\partial R} + \frac{\alpha}{R^4} - \frac{4\mu_L\dot{R}}{R}\right)$$

The variation in surface tension depends upon the variation in surface concentration of the surfactant Γ.

$$\frac{\partial\sigma}{\partial R} = \frac{\partial\sigma}{\partial\Gamma}\frac{\dot{\Gamma}}{\dot{R}} = \frac{-\chi}{\Gamma_o}\frac{\dot{\Gamma}}{\dot{R}} = \frac{2R_o^2\chi}{R^3} \quad \text{since} \quad 4\pi R^2\Gamma = 4\pi R_o^2\Gamma_o$$

so

$$\dot{\Gamma} = \frac{\partial}{\partial t}\left(\frac{R_o^2\Gamma_o}{R^2}\right) = \frac{-2R_o^2\Gamma_o\dot{R}}{R^3} \quad \text{where } \chi \text{ is defined as } -\frac{\partial\sigma}{\partial\Gamma}\Gamma_o$$

thus

$$\rho_L\left(R\ddot{R} + \frac{3}{2}\dot{R}_1^2\right) = \left(p_G(R,t) - p_\infty(t) - \frac{2\sigma}{R} - \frac{2\chi R_o^2}{R^3} - \frac{1}{R^3}\frac{\partial\alpha}{\partial R} + \frac{\alpha}{R^4} - \frac{4\mu_L\dot{R}}{R}\right) \tag{3.11}$$

Equation 3.11 is similar in form to those derived for the radial oscillations of ocean bubbles with organic film coatings (e.g. Glazman 1983). More advanced descriptions of the monolayer than the simple treatment expressed by Eq. 3.11 are available. For example, additional terms accounting for viscous dissipation in the surfactant layer may be included together with terms having a higher order dependence upon R^{-2} (Israelachvili 1991). The difficulty, however, is obtaining reliable experimental data from which the model parameters may be derived. For example, direct measurements of χ have been made for a variety of liquid-condensed and solid-state films (e.g. Joly 1972), but there is no data available for χ or α at frequencies in the MHz range. Predictions from molecular modelling are at present inadequate, and as mentioned earlier, in the absence of this data, Eqs. 3.8 and 3.11 are of equivalent value.

From Eq. 3.11 $$f_{Ss} = \frac{1}{R^3}\left(\frac{\alpha}{R} - 2\chi R_o^2 - \frac{\partial\alpha}{\partial R}\right) = \frac{1}{R^3}\left(\frac{k_1}{R} - k_2\right)$$

From Eq. 3.8 $$f_{Ss} = \frac{-4G_S(R_1 - R_{1e})\left(R_2^3 - R_1^3\right)}{R_2^3 R_1}$$

In the limit of negligible shell thickness this reduces to:

$$f_{Ss} = \frac{1}{R^3}\left(12G_S R_o^2 d_o\frac{R_e}{R} - 12G_S R_o^2 d_o\right) = \frac{1}{R^3}\left(\frac{k_1}{R} - k_2\right)$$

In spite of its potential for describing complex material behaviour Eq. 3.10 is also of limited value until functions $E_{1,2}$, etc. can be specified on the basis of reliable experimental data.

In order to improve the overall understanding of coated microbubble behaviour this lack of material data needs to be addressed. For coated microbubble design, however, it is a comparatively minor obstacle. The aim of the design process is to establish the optimum characteristics for a product and determine how these may be achieved. The absence of data for existing coated microbubbles is thus relatively insignificant, as demonstrated in the following section.

3.3.1.2 Designing the Shell

In order to meet the requirements for the ideal coated microbubble set out in Sect. 3.1.2, an improvement in coated microbubble detectability at low insonation pressures is needed. The most obvious means of achieving this would be to increase the harmonic content of the signal radiated by the microbubbles. The presence of harmonics in the coated microbubble signal is due to the fact that, for equal peak positive and negative insonation pressures, the amplitude of coated microbubble oscillations will be greater during expansion than during compression ($|R_{max}| > |R_{min}|$). Therefore, if the ratio R_{max}:R_{min} could be increased, the harmonic content and hence microbubble detectability could be enhanced. It is clear from the previous discussion that the most effective way of modify-

ing coated microbubble response is likely to lie with the encapsulating shell.

Both the structure and the material of the shell may be modified and there are a number of possible approaches. For example, the shell material may be selected or engineered so that the shear modulus G_s is smaller in tension than in compression. It would be inappropriate in an article of this length to include the rigorous modelling of this behaviour, and again such a demonstration would be of limited value given the lack of specific material data. The principle, however, can be demonstrated effectively using a much simpler model, of the type derived by Hoff et al. (2000), etc. for a shell of negligible thickness.

$$\rho_L\left(R\ddot{R}+\frac{3}{2}\dot{R}_1^2\right) = \left(p_o\left(\frac{R_o}{R}\right)^{3\kappa} - p_o - p_A\sin(\omega t) - \frac{2\sigma}{R} - \frac{12G_S R_o^2 d_o}{R^3}\left(1-\frac{R_e}{R}\right) - \frac{12\mu_S R_o^2 d_o \dot{R}}{R^4} - \frac{4\mu_L \dot{R}}{R}\right)$$

with G_S defined by $G_S(R_1) = \begin{cases} G_{Si}, R_1 \geq R_{e1} \\ G_{Sii}, R_1 < R_{e1} \end{cases}$

The frequency spectra for the pressure radiated by coated microbubbles having $G_{sii} = G_{si}$ and $G_{sii} = x\, G_{si}$ under identical insonation conditions is shown in Fig. 3.4 for various values of x. As may be seen, there is a distinct enhancement in the harmonic content when $x > 1$. There are a number of materials which naturally display this behaviour. The response of TiNi crystals, for example, has long been recognised as being asymmetric in tension and compression (Gall et al. 1999). Clearly this type of material is unsuitable for coating microbubbles, but similar behaviour has also been demonstrated for materials such as cartilage (Provenzano et al. 2002) and other natural polymers. The reported tensile and compressive moduli are derived from relatively large samples and may relate to material structure on a scale which is large compared with the thickness of a microbubble coating. However, it may be possible to imitate these structures on a much smaller scale. The inclusion of cholesterol molecules in a cell membrane for example has been shown to produce a highly non-linear increase in its resistance to deformation (Boal 2002). Since the coatings of phospholipid-coated microbubbles are very similar in composition to cell membranes, it is perfectly feasible that they could be similarly engineered.

There are alternative means by which enhanced non-linear behaviour may be achieved. The shell may be constructed so that it will buckle in compression, for example by varying its thickness over the coated microbubble surface. This will have a similar effect to increasing the ratio of compressive to tensile modulus, since a buckled shell will not compress to the same degree as one which remains smooth. Similarly, it is easy to envisage various ways in which the shell structure may be designed to alter its relative resistance to tension and compression that would be easily within the capabilities of available manufacturing methods.

3.3.2 The Insonating Field

As indicated in Figs. 3.3 and 3.4, variation in the US field parameters will have a strong impact on coated microbubble behaviour (Simpson et al. 1999; Uhlendorf and Hoffmann 1994). It will also affect the quality of the scan image directly, in terms of resolution, etc. Both the nature of the input waveform and its propagation through the microbubbles' surroundings must be taken into account.

3.3.2.1 Influence of the Field Parameters

Provided the thickness and viscosity of the encapsulating shell is not too great compared with their diameter, coated microbubbles will resonate at a specific frequency. The most appropriate range of frequencies for a given application will thus depend strongly upon the size distribution of the coated microbubble population, and either the incident spectrum must be selected accordingly or it may be desirable to control the size of the coated microbubbles to enable a particular frequency range to be used, e.g. to achieve a particular level of resolution.

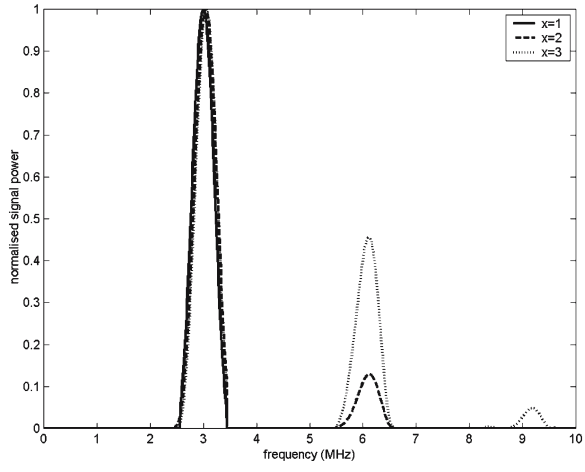

Fig. 3.4. Frequency spectra for the pressure radiated by coated microbubbles insonated at 3 MHz and 50 kPa with shells of varying degrees of non-linearity

Resonance, however, is not the only consideration in the selection of the insonation frequency. A number of methods have been investigated with the aim of improving image quality by manipulation of the input spectrum. One of the most common is to use a combination of two frequencies in order to generate an enhanced response at the difference frequency. Various different versions of this technique have been developed (Wyzalkowski and Szeri 2003). The use of coded excitation ("chirps") has also been examined (Borsboom et al. 2003). The imaging strategies which have been developed to take advantage of these techniques will be reviewed in subsequent chapters.

The amplitude of the incident field is also a significant factor. As mentioned earlier, it will determine the degree of non-linear behaviour exhibited by existing coated microbubbles and is clearly important in terms of coated microbubble destruction. It is also likely to be a factor in determining the fraction of a coated microbubble population activated by the incident field. The maximum and minimum pressures which may be used for an ultrasound scan are limited by considerations of patient safety and signal attenuation respectively. The aim in improving coated microbubble design is to minimise the insonation pressure required to obtain the desired image quality.

3.3.2.2 Influence of the Surrounding Fluid

Between transmission and detection, the incident and scattered fields must propagate through the surrounding tissue and will inevitably be modified to some extent in the process. Whilst it has been assumed that the effects of compressibility will be small in terms of coated microbubble dynamics, they may have a greater impact on the propagation of the sound field. During compression, the local density of the tissue is increased slightly and so too therefore is the speed at which the wave travels through it. The reverse occurs during rarefaction, with the result that the shape of the wave or pulse, in the case of imaging, will be distorted. This distortion corresponds to an increase in the harmonic content of the frequency spectrum and will affect both the response of the coated microbubbles and the degree to which the pulse is attenuated. Thus, to achieve a particular coated microbubble response and signal amplitude, this effect must be taken into account.

The compressibility of the surrounding fluid must also be included when a population rather than a single coated microbubble is considered. For the reasons given in Sect. 3.2.1, acoustic radiation damping is a small effect for a single coated microbubble at low insonation power, particularly if the viscosity of the shell is relatively large and thus forms the main contribution to the overall damping. In a coated microbubble population, however, the presence of the other coated microbubbles can increase the effective compressibility of the surroundings considerably, and also introduces the problem of multiple scattering between microbubbles. At sufficiently low concentrations it is still reasonable to neglect acoustic damping and predict the overall acoustic signal by linear summation of single coated microbubble responses, assuming that the activated proportion of the population is known. At higher concentrations, however, and importantly in the range corresponding to coated microbubble injections, it has been shown experimentally that linear summation fails to accurately predict acoustic response (Marsh et al. 1997).

3.3.3 The Filling Gas

It was assumed in deriving Eq. 3.8 that the filling gas would behave polytropically, on the basis that the pressure inside the coated encapsulating at low amplitudes of oscillation would be relatively low compared with the critical pressure for the gas. This assumption is valid for air and many other gases (Cengel and Boles 1989), although it should not be made automatically for every gas. It was also assumed that the gas behaviour would be isothermal (κ=1). Given the high specific heat capacity of plasma and the small size of the coated microbubble, it is reasonable to assume that the surrounding fluid will behave as a heat sink and that the temperature gradient within the coated microbubble will be very small at low insonation pressures (Neppiras 1980). Moreover, it was determined subsequently that microbubble response was relatively insensitive to the value of κ (Fig. 3.3).

The choice of filling gas will also affect the long term stability of the coated microbubble. If the shell is gas permeable and/or soluble, then the rate at which the coated microbubble dissolves will depend upon the solubility of the gas as well as the durability of the shell. Clearly, any shrinkage of the coated microbubbles due to dissolution will affect their acoustic response and this may be important for some applications. In addition there may be some safety issues relating to very low solubility gases. If free bubbles

are able to persist after the microbubble shells have degraded they could potentially coalesce to form a relatively large bubble capable of causing an embolism. Finally, the possibility of chemical interaction between the filling gas and the shell material or any therapeutic compounds may need to be considered.

3.4 Concluding Remarks

Advances in imaging technology, and more recently in therapeutic applications, such as drug delivery, have greatly increased the range of potential benefits offered by ultrasound contrast agents. Hence, the need to develop agents for specific tasks has also increased. The aim of this chapter has been to present an overview of how contrast agents may be designed in order to improve their suitability for particular applications. It has been shown that analytical techniques may be applied to identify the most important factors for modelling and design, and that this knowledge may be employed to modify coated microbubbles behaviour.

There are still some areas of uncertainty. The characterisation of existing agents is currently unsatisfactory and there is undoubtedly scope for improvement in the modelling of contrast agent behaviour in vivo. Even using existing knowledge, however, there are considerable advantages to be gained through coated microbubble design. In the example given, it was shown how the material and/or structure of the encapsulating shell could be selected in order to enhance the non-linearity of coated microbubble oscillations at low insonation pressures. Similar improvements may be achieved by appropriate selection of the filling gas to control coated microbubble longevity, and coated microbubble structure may be modified to improve targeting. More and more benefits will be realised as the deficiencies in the existing theory are addressed.

References

Allen J, Roy R (2000) Dynamics of gas bubbles in viscoelastic fluids II. Non-linear viscoelasticity. J Acoust Soc Am 108:1640-1650

Boal D (2002) Mechanics of the cell, 1st edn. Cambridge University Press, Cambridge

Borsboom J, Chin C, de Jong N (2003) Non-linear coded excitation method for ultrasound contrast imaging. Ultrasound Med Biol 29:285-292

Cengel Y, Boles M (1989) Thermodynamics: an engineering approach. Ultrasound Med Biol 29:1749:1757

Church C (1995) The effects of an elastic solid surface layer on the radial pulsations of gas bubbles. J Acoust Soc Am 97:1510-1520

De Jong N, Hoff L, Skotland T, Bom N (1992) Absorption and scatter of encapsulated gas filled microspheres: theoretical considerations and some measurements. Ultrasonics 30:95-103

Duck F (1990) Physical properties of tissue: a comprehensive reference book, 1st edn. Academic, London

Flynn H (1964) Physics of acoustic cavitation in liquids. In: Mason W (ed) Physical acoustics 1B. Academic, London

Fox F, Herzfeld J (1954) Gas bubbles with organic skin as cavitation nuclei. J Acoust Soc Am 26:984-989

Gall K, Sehitoglu H, Chumlyakov Y, Kireeva I (1999) Tension compression asymmetry of the stress-strain response in aged single crystal and polycrystalline NiTi. Acta Mater 47:1203-1217

Glazman R (1983) Effects of adsorbed films on gas bubble radial oscillations. J Acoust Soc Am 74:980-986

Gorce J, Arditi M, Schneider M (2000) Influence of bubble size distribution on the echogenicity of ultrasound contrast agents: a study of SonoVue. Invest Radiol 35:661-671

Gramiak R, Shah PM (1968) Echocardiography of the aortic root. Invest Radiol 3:356-366

Green E, Rivlin R (1957) The mechanics of non-linear materials with memory. Arch Rational Mech Anal 1:1-21

Hoff L, Sontum P, Hovem J (2000) Oscillations of polymeric microbubbles: Effect of the encapsulating shell. J Acoust Soc Am 107:2272-2280.

Israelachvili J (1991) Intermolecular and surface forces, 2nd edn. Academic, London

Joly M (1972) Rheological properties of monomolecular films, part II. Experimental results, theoretical interpretation and applications. In: Matijevic E (ed) Surface colloid science. Wiley, New York, pp 79-194

Khismatullin D, Nadim A (2002) Radial oscillations of encapsulated microbubbles in viscoelastic liquids. Phys Fluids 14:3534-3557

Leighton T (1994) The acoustic bubble, 1st edn. Academic, London

Lord W, Ludwig R, You Z (1990) Developments in ultrasonic modelling with finite element analysis. J Non Destruct Eval 9:129-139

Marsh J, Hall C, Hughes M (1997) Broadband through-transmission signal loss measurements of Albunex® suspensions at concentrations approaching in vivo doses. J Acoust Soc Am 101:115-1161

Morgan K, Allen J, Chomas J, Dayton P, Ferrara K (1999) Experimental and theoretical analysis of individual contrast agent behavior. IEEE Proc Ultrason Symp 2:1685-1688

Neppiras E (1980) Acoustic cavitation. Phys Rep (Phys Lett) 61:159-251

Nyborg W (2001) Biological effects of ultrasound: development of safety guidelines, part II. General review. Ultrasound Med Biol 27:301-333

Postema M, Bouakaz A, Chin C, de Jong N (2003) Simulations and measurements of optical images of insonified ultrasound contrast microbubbles. IEEE Trans Ultrason Ferr Freq Cont 50:523-535

Provenzano P, Lakes R, Corr D, Vanderby R Jr (2002) Application of non-linear viscoelastic models to describe ligament behaviour. Biomech Mod Mechanobiol 1:45-57

Simpson DH, Chin C, Burns P (1999) Pulse inversion Doppler: a new method for detecting non-linear echoes from microbubble contrast agents. IEEE Trans Ultrason Ferr Freq Cont 46:372-382

Stride E, Saffari N (2003) The destruction of microbubble ultrasound contrast agents. Ultrasound Med Biol 29:563-573

Stride E, Saffari N (2004) Theoretical and experimental investigation of the behaviour of ultrasound contrast agent particles in whole blood. Ultrasound Med Biol 30(11):1495–1509

Uhlendorf V, Hoffmann C (1994) Non-linear acoustic response of coated microbubbles in diagnostic ultrasound. Proc IEEE Symp Ultrason 2:1559-1562

Wyzalkowski M, Szeri A (2003) Optimization of acoustic scattering from dual frequency driven microbubbles at the difference frequency. J Acoust Soc Am 113:3073-3079